

# ESTIMATION OF BANDLIMITED GRAYSCALE IMAGES FROM THE SINGLE BIT OBSERVATIONS OF PIXELS AFFECTED BY ADDITIVE GAUSSIAN NOISE

Abhinav Kumar and Animesh Kumar

Department of Electrical Engineering  
Indian Institute of Technology Bombay  
Mumbai, India – 400076  
[abhinavkumar,animesh]@ee.iitb.ac.in

## ABSTRACT

The estimation of grayscale images using their single-bit zero mean Gaussian noise-affected pixels is presented in this paper. The images are assumed to be bandlimited in the Fourier cosine transform (FCT) domain. The images are oversampled over their Nyquist rate in the FCT domain. We propose a non-recursive approach based on first order approximation of Cumulative Distribution Function (CDF) to estimate the image from single bit pixels which itself is based on Banach's contraction theorem. The decay rate for mean squared error of estimating such images is found to be independent of the precision of the quantizer and it varies as  $O(1/N)$  where  $N$  is the "effective" oversampling ratio with respect to the Nyquist rate in the FCT domain.

**Index Terms**— Estimation, Bandlimitedness, Images, FCT, Binary Pixels.

## 1. INTRODUCTION

We explore the image estimation from their noise-affected single bit pixels in this paper. There have been a few attempts to address this problem. Optics based approach [1] has been used to recreate the images from one or two binary images. However, Banach's Contraction Theorem [2], [3] or linearisation based approach is not used. Also, no previous work gives a bound on the distortion (mean-squared error between estimated and original image) of the reconstructed images.

There have been a few works in the area of 1-D signal processing. Reconstruction of 1-D continuous signals has been done from the signed noisy samples using a random process as dither [4]. A mean squared error of  $O(1/N^{2/3})$  was obtained where  $N$  is the oversampling factor with respect to the Nyquist rate. One dimensional continuous bandlimited signals were recovered using Picard's Iterations when such signals were "companded" by an another signal [5]. The "quantizer precision indifference principle" of the distortion encountered while reconstructing Zakai-class [6] bandlimited 1-D signals from noisy samples has been carried out [7],[8].

The distortion was found to vary as  $O(1/N)$  and was independent of the precision of the quantizer i.e. the presence of noise and precision of the quantizer only decides the proportionality constant of the distortion. This work essentially extends their recursive scheme to images. Their scheme is also simplified based on the CDF linearisation. Also the filtering is carried out in FCT domain instead of the traditional Fourier domain.

The key contribution of the paper is as follows. If  $N$  is the "effective" oversampling factor with respect to the Nyquist rate of a grayscale image in the FCT domain, then a distortion of  $O(1/N)$  can be achieved irrespective of the quantizer precision.

## 2. BACKGROUND

### 2.1. Fourier Cosine Transform

The 1-Dimensional FCT and 1-D Inverse Fourier Cosine Transform (IFCT) [9] for even signal  $f(t)$  are defined by (1)

$$F(\omega) = 2 \int_0^{\infty} f(t) \cos(\omega t) dt; f(t) = \frac{2}{\pi} \int_0^{\infty} F(\omega) \cos(\omega t) d\omega \quad (1)$$

The interpolation of samples in time domain happens to be a low-pass filtering operation in frequency-domain. The interpolation kernel for the signal samples is then  $f(t) = \frac{2}{\pi} \int_0^{\omega_m} 1 \cdot \cos(\omega t) d\omega = \frac{2}{\pi} \frac{\sin(\omega_m t)}{t}$ , which is a sinc function. Thus, the interpolation function for the FCT is same as the interpolation function for the Fourier Transform. This kernel is not absolutely summable and hence we go for a bandlimited absolutely summable kernel. The FCT of the kernel  $\phi(t)$  is shown in Fig. 1. Clearly, for continuous frequency response  $\Phi(\omega)$ , we should have  $\lambda > 1$ . The closed form expression of  $\phi(t)$  [7] is then given by

$$\phi(t) = \begin{cases} 1 + \frac{a}{\pi} \\ \frac{\sin((\pi+a)t) \sin(at)}{at^2} \end{cases}, t = 0 \quad (2)$$

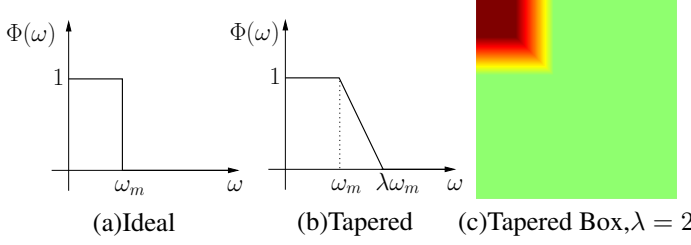


**Fig. 1:** Low Pass Filters in frequency domain.

where  $a = \frac{\lambda-1}{2}$ .

Images have been shown to be better bandlimited in Cosine Transform Domain than in Fourier Transform Domain [10],[11]. Most of the energy of the images are contained in the upper left corner of the images [12]. The filter to be used should be a product of two  $\phi$  kernels. The closed form expression of  $\phi(x, y)$  is given by  $\phi(x, y) = \phi(x)\phi(y)$ . The filter  $\phi(x, y)$  acts as a low pass filter for images. The frequency response of  $\phi(x, y)$  denoted by  $\Phi(\omega_1, \omega_2)$  is shown in the Fig. 1c.

## 2.2. Image and Noise Model

We consider images  $g(x, y)$  to be bandlimited in Zakai sense [6] in FCT domain i.e., there exists a  $\phi(x, y; \omega_m, \omega_m)$  such that  $g(x, y) * \phi(x, y; \omega_m, \omega_m) = g(x, y)$  where  $*$  denotes the linear convolution operation. Here,  $\phi(x, y)$  is called the kernel function and  $(\omega_m, \omega_m)$  is the cutoff frequency in FCT domain. The other requirement is that image is bounded. In other words,  $|g(x, y)| \leq 1$ . The image is corrupted by a zero mean additive Gaussian noise  $W$  of variance  $\sigma^2$ .

## 2.3. Sampling Model

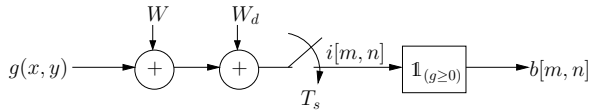


**Fig. 2:** Sampling Scheme for single bit precision pixels.

The indicator function models the single bit thresholding operation of the image pixels in Fig. 2.  $W_d$  and  $T_s$  denote the dither noise and the sampling rate respectively. We also generalise the concept of Nyquist sampling rate from Fourier transform to FCT domain. Let  $f_m$  be the maximum frequency content of a 1-D signal in FCT domain. Then, the sampling rate for perfect reconstruction  $> 2f_m$ . If we oversample a signal  $N$  times its Nyquist rate along each of the axes, then the sampling rate is  $N2f_m$ .

Distortion measure  $D$  considered for the images is mean-squared error i.e.  $D = \frac{1}{M} \sum_x \sum_y [\hat{g}(x, y) - g(x, y)]^2$ , where

$g(x, y)$  and  $\hat{g}(x, y)$  denote the original and estimated images respectively and  $M$  is total number of pixels in the image.

## 3. IMAGE ESTIMATION ALGORITHMS

This section contains the image estimation algorithms using full precision as well as binary pixels.

### 3.1. Estimating Bounded Zakai Sense bandlimited Images from Full Precision Pixels

We first interpolate the noisy sampled pixels  $i[m, n]$  (Fig. 2) to get the image

$$h(x, y) = \sum_{m \in \mathbb{Z}} \sum_{n \in \mathbb{Z}} i[m, n] \phi\left(\frac{x - mT_s}{T_s}, \frac{y - nT_s}{T_s}\right) \quad (3)$$

Then, the estimate of the original image  $g(x, y)$  is obtained by low passing the image  $h(x, y)$  as

$$\hat{g}(x, y) = h(x, y) * \phi(x, y; \omega_m, \omega_m) \quad (4)$$

### 3.2. Estimating Bounded Zakai Sense bandlimited Images from Binary Pixels

If a constant signal  $c$  corrupted by Gaussian noise with mean zero and variance  $\sigma^2$  is observed through single bit quantisers, the mean of the observations converges to  $\mathcal{C}(c)$  [7] where  $\mathcal{C}(t)$  denote the CDF of the Gaussian noise.

Here, we are given the noisy binary pixels  $b[m, n]$  (Fig. 2) sampled at above the Nyquist rate with values as 1 or 0 and thresholded at 0. The sampling rate ( $T_s$ ), oversampling factor ( $N$ ), steepness factor ( $\lambda$ ) and variance of the zero mean Gaussian noise ( $\sigma^2$ ) as well as the dither ( $\sigma_d^2$ ) are assumed to be known. Let  $\mathcal{C}(t)$  denote the CDF of the Gaussian random variable  $\mathcal{N}(0, \sigma^2 + \sigma_d^2)$ .

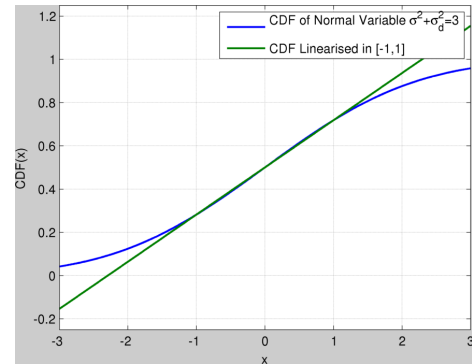


**Fig. 3:** CDF of zero mean Gaussian random variable and its linearised approximation around  $[-1, 1]$ .

Interpolation of binary pixels gives us  $H_N(x, y)$ . Following the procedure of statistical indifference [7], it can be

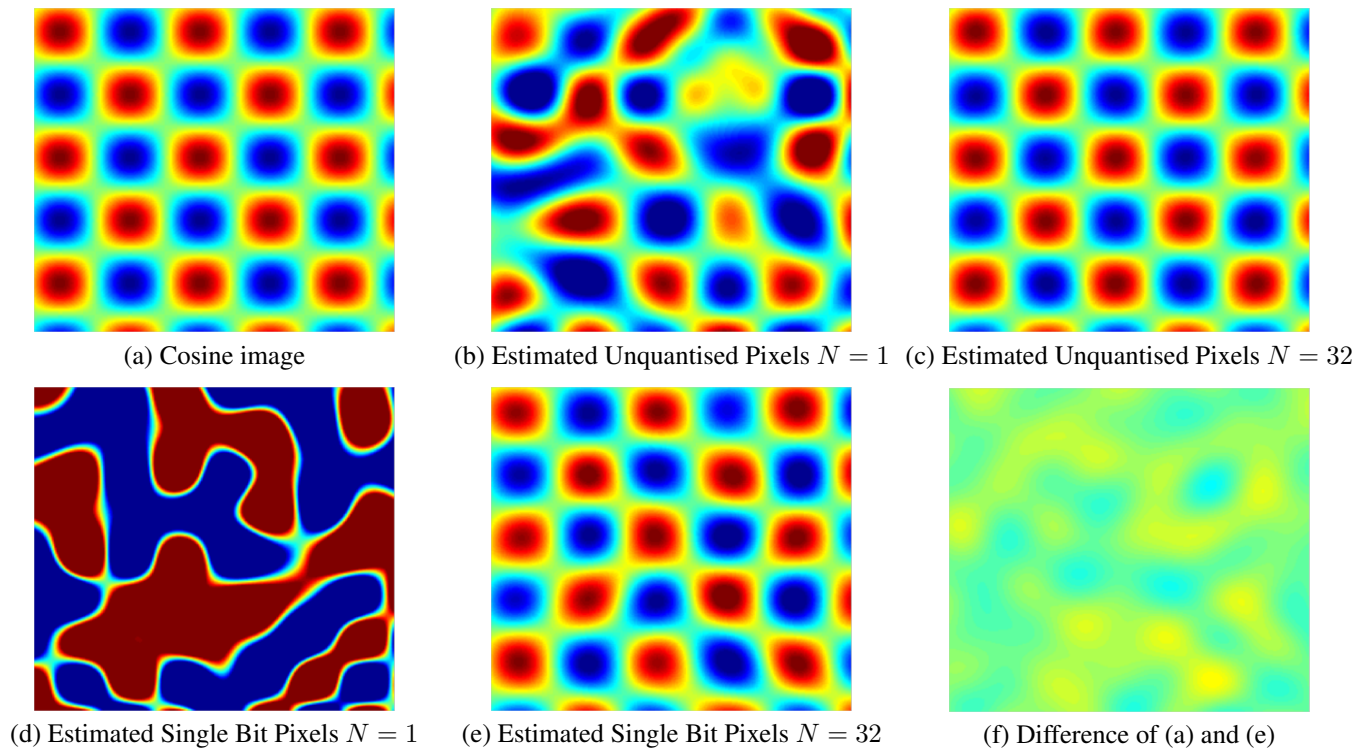


**Fig. 4:** Estimation of synthetic Cosine image using Unquantised and Single Bit Pixels.

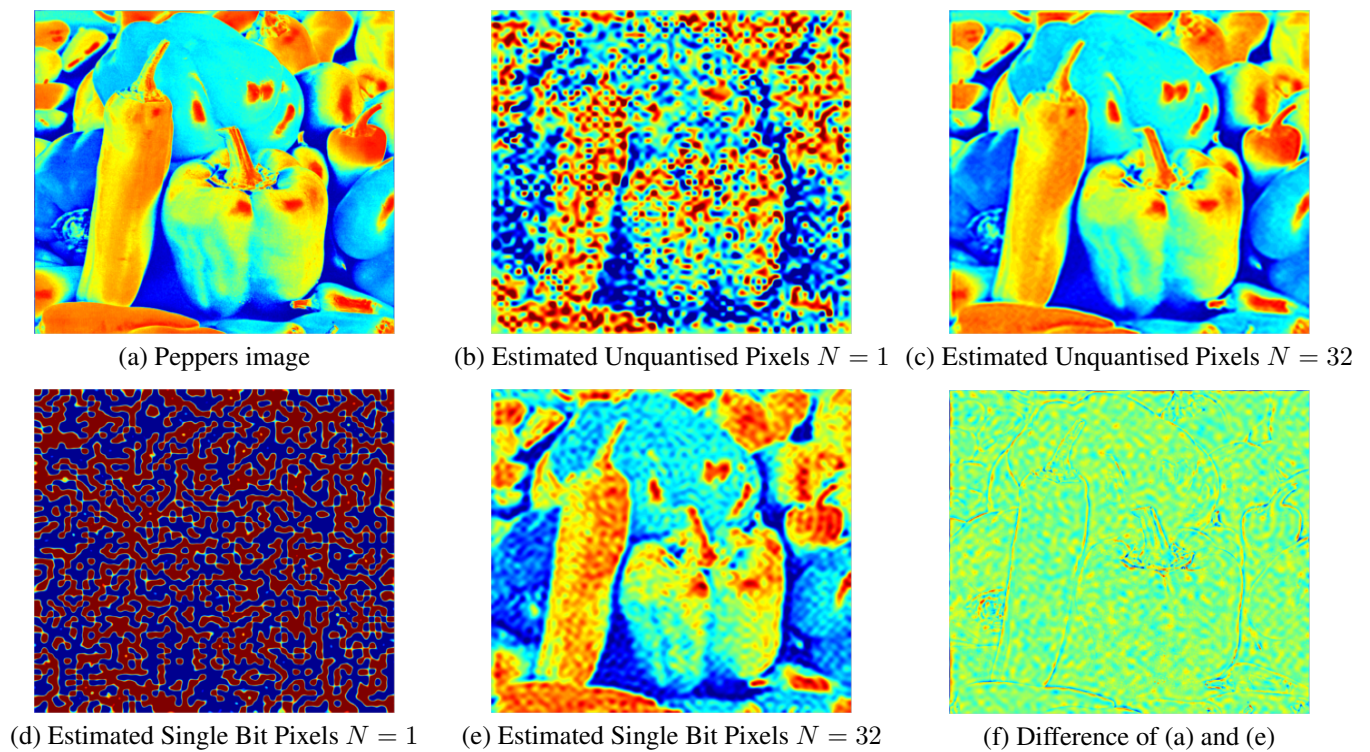


**Fig. 5:** Estimation of Peppers image using Unquantised and Single Bit Pixels.

shown to converge to  $\mathcal{C}(g(x, y)) * \phi(x, y; \omega_m, \omega_m)$  which is a non-linear estimate of  $g(x, y)$ . If a dither Gaussian noise of large variance is added before sampling, the CDF of the Gaussian random variable is nearly linear in the range  $[-1, 1]$ . Fig. 3 shows the plot of CDF of Gaussian random variable and its first order approximation in the region  $[-1, 1]$ . Clearly, as the variance of the Gaussian random variable increases, the approximation of CDF by a straight line becomes more and more perfect. Hence, the estimate is of the form  $\alpha g(x, y) + \beta$ .

Now, CDF can be directly inverted without any clipping or recursion to obtain the original image  $g(x, y)$  back. Then, the direct algorithm 1 is used to recover  $g(x, y)$ .

---

**Algorithm 1** Non-Recursive Image Denoising Algorithm using Single Bit Pixels

---

**Require:**  $g(x, y)$

$$H_N(x, y) \leftarrow \sum_{m \in \mathbb{Z}} \sum_{n \in \mathbb{Z}} (2b[m, n] - 1) \phi\left(\frac{x - mT_s}{T_s}, \frac{y - nT_s}{T_s}\right) * \\ \phi(x, y; \omega_m, \omega_m) \\ \alpha \leftarrow \frac{\mathcal{C}(1) - \mathcal{C}(-1)}{2} \\ \hat{g}(x, y) \leftarrow \frac{H_N(x, y)}{2\alpha}$$


---

## 4. RESULTS

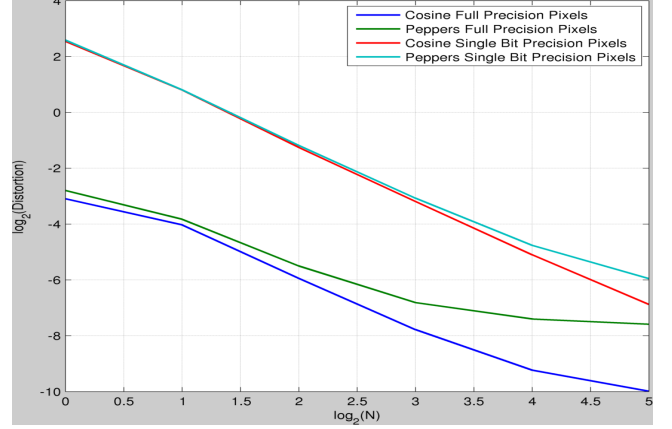
We consider two images for our simulations- a synthetic Cosine image  $Z = \cos(2\pi f_m x) \cos(2\pi f_m y)$  and a real Peppers image. The synthetic image is already in the range  $[-1, 1]$  while the real image is initially converted to grayscale image in the range  $[0, 255]$  which is then scaled in the range  $[-1, 1]$ . The number of DCT coefficients was  $72 \times 72$  for all simulations which corresponds to  $f_m = 4$  Hz on both the axes. The steepness factor  $\lambda$  has been kept at 2 and the noise variance  $\sigma^2$  for all images was 0.1. The dither variance  $\sigma_d^2$  was 2.9. The spatial grid for  $2048 \times 2048$  image for each of the axes has been kept as  $-2.5575 : .0025 : 2.56$  respectively. Denoising from single bit precision pixels was carried out using the non-recursive algorithm 1.

Fig. 4 and 5 shows the estimation of  $2048 \times 2048$  images with infinite and single bit quantizer precision for the two images respectively at different oversampling factors  $N$  along each of the axis.

The plot of log of distortion for the two  $2048 \times 2048$  images versus log of the oversampling factor for the full precision and single bit precision case is shown in Fig. 6.

### 4.1. Discussions

The loss due to quantization is constant across oversampling factors for different images which is evident in Fig. 6. The slope of the plot of log of distortion with log of oversampling factor for single bit precision samples in Fig. 6 is  $-2$  which shows that distortion decreases as  $O(1/N^2)$ . The effective



**Fig. 6:** Plot of log of Distortion with log of oversampling factor along each axes  $N$  for  $2048 \times 2048$  images.

number of samples in the region is  $N^2$  since we are oversampling each axis by  $N$ . Also, the distortion gap for unquantised and quantised estimation is constant at different  $N$ .

The slope of the plot of log of distortion with log of oversampling factor for full precision samples will become more accurate at the cost of computational resources.

Some of the edges (which are high pass in nature) are not recovered back because of the low pass nature of the kernel function. The distortion due to such out of band component  $D_{outofband}$  adds up linearly to the distortion caused due to reconstruction. Hence, for real images, we have  $D_{observed} - D_{outofband}$  varies as  $O(1/N)$ .

## 5. CONCLUSIONS

The estimation of images from infinite bit precision and single bit pixels has been worked out for 2-D grayscale images. However, the results seem astonishing in the sense that an image can be estimated just by using the single-bit pixels. The tradeoff lies between the number of bits of quantizer precision and the oversampling introduced. The distortion for the reconstruction varies as  $O(1/N)$  for images which is independent of the precision of the quantizer where  $N$  is the effective oversampling ratio.

## 6. FUTURE WORKS

Quantizer precision indifference principle can be extended to setups where basis is not ordered such as Wavelets and Contourlets. It would be interesting to see how this procedure behaves when we couple it with Compressing Sensing Algorithms and the edge preserving priors. Estimation without using dither when the CDF is non-linear in the range  $[-1, 1]$  would also be a good territory to explore.

## Acknowledgments

The authors would like to thank Nikunj Patel and Saurabh Kumar for discussions on this topic. Nikunj was also kind enough to allow the simulations run on the TI-DSP lab machines. Saurabh was patient enough in listening to several problems.

## 7. REFERENCES

- [1] Rafael Hostettler, Ralf Habel, Markus Gross, and Wojciech Jarosz, “Dispersion-based color projection using masked prisms,” *Computer Graphics Forum (Proceedings of Pacific Graphics)*, vol. 34, no. 7, Oct. 2015.
- [2] Erwin Kreyszig, *Introductory functional analysis with applications*, vol. 81, Wiley New York, 1989.
- [3] Robert M Brooks and Klaus Schmitt, *The contraction mapping principle and some applications*, Department of Mathematics, Texas State University, 2009.
- [4] Elias Masry, “The reconstruction of analog signals from the sign of their noisy samples,” *Information Theory, IEEE Transactions on*, vol. 27, no. 6, pp. 735–745, 1981.
- [5] HJ Landau and WL Miranker, “The recovery of distorted band-limited signals,” *Journal of Mathematical Analysis and Applications*, vol. 2, no. 1, pp. 97–104, 1961.
- [6] Moshe Zakai, “Band-limited functions and the sampling theorem,” *Information and Control*, vol. 8, no. 2, pp. 143–158, 1965.
- [7] Animesh Kumar and Vinod M Prabhakaran, “Estimation of bandlimited signals in additive gaussian noise: a” precision indifference” principle,” *arXiv preprint arXiv:1211.6598*, 2012.
- [8] Animesh Kumar and Vinod M Prabhakaran, “Estimation of bandlimited signals from the signs of noisy samples,” in *Acoustics, Speech and Signal Processing (ICASSP), 2013 IEEE International Conference on*. IEEE, 2013, pp. 5815–5819.
- [9] K Ramamohan Rao and Ping Yip, *Discrete cosine transform: algorithms, advantages, applications*, Academic press, 2014.
- [10] Rafael C Gonzalez and Richard E Woods, *Digital image processing*, Prentice hall Upper Saddle River, 2002.
- [11] Anil K Jain, *Fundamentals of digital image processing*, Prentice-Hall, Inc., 1989.
- [12] Nasir Ahmed, T Natarajan, and Kamisetty R Rao, “Discrete cosine transform,” *Computers, IEEE Transactions on*, vol. 100, no. 1, pp. 90–93, 1974.